Optimized ohmic contacts for InAlGaN/GaN HEMTs

Pierre Ruterana, Marie Pierre Chauvat, Magali Morales, Farid Medjdoub, Piero Gamarra, Christian Dua, Sylvain Delage

Optimized ohmic contacts for InAlGaN/GaN HEMTs

Pierre Ruterana[1], Marie-Pierre Chauvat[1], Magali Morales[1], Farid Medjdoub[2], Piero Gamarra[4], Christian Dua[3] and Sylvain Delage[3]

1. CIMAP, 6 boulevard du Marechal Juin, Université de Caen, Caen, France
2. Institute of Electronics, Microelectronics and Nanotechnology (IEMN), Av. Poincaré,Villeneuve d'Ascq, France
3. III-V Lab, 1 Avenue Augustin Fresnel, Campus Polytechnique, Palaiseau, France
4. On leave of III-V Lab, 1 Avenue Augustin Fresnel, Campus Polytechnique, Palaiseau, France

In this work, we have carried out a detailed transmission electron microscopy investigation on ohmic contacts in InAlGaN/GaN high electron mobility transistors consisting of Ti/Al/Ni/Au deposited by evaporation electron beam followed by a rapid thermal annealing at 875°C for 30s under N2 atmosphere. Subsequent to an optimized surface preparation, prior to the metal deposition, it has been possible to systematically obtain a contact resistance of 0.15-0.16 Ω*.mm instead of the usual 0.5-0.6* Ω*.mm. This is comparable to the state of the art results which have been published subsequent to more complex processes including molecular beam regrowth.*

1. Introduction

For the fabrication of high electron mobility transistors (HEMTs), the lattice matched InAlN/GaN system offers many advantages due to the possibility to obtain strain free devices and a high density two dimensional gas [1]. As has been reported, HEMTs with an InAlN barrier may operate at very highest frequencies (~ 300 GHz) and withstand temperatures of 1000 °C [2]. To this end, the gate length should be smallest for such performances; and parasitic resistances and short channel effects need to be avoided. The main contribution to the parasitic resistance comes from the access and contact resistance [3]. More specifically, the contact resistance should be as small as possible; latterly, a number of works have applied additional and complex steps during the process, such as molecular beam epitaxy regrowth, in order to bring the contact resistance to below 0.5 Ω.mm [4]. The ohmic contacts on wide band gap nitrides have been optimized on n type GaN [5], but things can be more complicated for AlGaN or InAlN in HEMTs heterostructures, as the band gap becomes large. The standard scheme implies the Ti/Al/Mx/Au multilayer which is deposited on a specifically prepared surface of the HEMT heterostructure with subsequent thermal annealing for alloying. Each of the metals plays a specific role. Mx (Ti, Ni, Mo, Pt) is a metal intended to play the role of blocking layer from in and out diffusion of Au and Al, respectively. Au is deposited in order to protect the system from oxidation. As per the enthalpies of formation −110.9, −265.5, and −318.1 kJ/mol of GaN, TiN, and AlN, Ti will tend to break the Ga-N bond and lead to the formation of an n^+ doped surface area rich in nitrogen vacancies. This creates donor states just below the conduction band minimum and pins the Fermi level leading to the formation of a tunnel junction towards the two dimensional electron gas responsible for the ohmic contact. The annealing is usually carried out under a nitrogen atmosphere thus helping towards the formation of an interfacial TiN layer which is a thermally stable compound and has a low contact resistance to GaN [5, 6]. Depending

on the annealing conditions the reaction can lead to degradation of the GaN superficial layer with formation of voids underneath the TiN thin layer [7]. The use of the Ti/Al sequence is commonly preferred where the relative thicknesses have been optimized for GaN [8] and AlGaN [9], as well as the annealing temperatures for lowest contact resistance around 850-900°C, rapid thermal annealing [9]. In these systems, the metallic layers thickness, the barrier surface defects, the annealing temperature affect the contact resistance and surface morphology [10]. Moreover, the barrier surface constitutes the termination of the crystallographic defects that come from the underlying layers such as threading dislocations [11], inversion domains [12] or stacking faults [13,14]. Such defects, in particular the threading dislocations, may affect the reaction during the contact annealing step [15]. In the case of InAlN or InAlGaN, the standard values of ohmic contacts are around 0.5-0.6 Ω.mm. In order to bring the ohmic contact below 0.2 Ω.mm, complex processes have involved localized molecular beam regrowth of n+ doped GaN prior to metal deposition [16], recess to decrease the AlInN thickness in combination with specific surface treatment [17].
In the following, we report on our transmission electron microscopy investigation during the optimization of the Ti/Al/Ni/Au ohmic contact on InAlGaN/Al/GaN. Apart from the more conventional contact resistance of 0.5 -0.6 Ω.mm, we discuss the evolution of the microstructure, when values of 0.15 Ω.mm are systematically attained through an optimized surface treatment.

2. Experiments methods

The epitaxial HEMT structure of SiC (substrate) /AlN(nucleation) /GaN(template) /AlInGaN (barrier) was carried out by Metal Organic Vapor Phase Epitaxy (MOVPE) on (0001) SiC substrates. Firstly, a 100-nm-thick AlN nucleation layer was deposited, followed by 2µm GaN template and an ultrathin AlN spacer layer (1.2nm); finally a 6nm thick $In_{1-x}Al_x(Ga)N$ barrier layer. The sample was covered then by a SiN passivation layer. To deposit the ohmic contact, it was necessary to remove the passivation layer and apply an optimized chemical surface treatment based on B and Cl gases. The deposition of metal stack [Ti/Al/Ni/Au (12/200/40/50 nm)] was carried out by electron beam evaporation as a first step to fabricate the ohmic contact, followed by rapid thermal annealing at 875°C for 30s in N_2 atmosphere to insure the alloying for contact. The metals used for the gate were the Ni/Au. The final contact resistance has been extracted by transmission line measurement (TLM). This TEM results on this optimization are compared to those obtained on an industrial standardized process for the multilayer stack of Ti(10)/Al(100)/Ni(40)/Au(10)/Ti(10)/Pt(50). In this instance, contact resistances between 0.3 and 0.6 Ω.mm are measured.
The samples for Transmission Electron microscopy (TEM) were prepared in cross-section using a focused ion beam (FIB). The chemical analysis and atomic scale investigations were carried out in a Scanning TEM (a cold field emission gun Jeol ARM microscope) which is double corrected for the aberrations of the probe and objective lens. It is also equipped with a large Si-Li (1 steradian) detector for energy dispersive spectroscopy (EDS) and an electron energy loss spectrometer.

3. Results

The list of the investigated sample series is shown in Table 1 for the representative four ones as related to the lowest measured corresponding contact resistance. Clearly, three values of contact resistance are noticeable, above 0.5 Ω.mm correspond the standard values that are seen in the literature, and in the 0.3-0.4 Ω.mm range which have at times been cited as record

values [18] for contact to InAlN. For the S4 sample, this 0.15 Ω.mm is comparable to Rc values which have been reported subsequent to recess and regrowth of n+ GaN at source and drain areas for instance by MBE [4, 16].

In this investigation, the samples exhibit very different microstructures, which brings up questions for the possible mechanisms, which may govern the ohmic behaviour of the corresponding devices.

Sample	Barrier	Treatment	Multilayer	Thickness (nm)	Rc (Ω.mm)
S1	InAlGaN	Standard	Ti/Al/Ni/Au/Ti/Pt (10,100,50,40,10,10 nm)	220	**0.56**
S2	InAlGaN	Standard	’’	220	**0.37**
S3	InAlGaN	Standard	Ti/Al/Ni/Au (12,200,40,50 nm)	302	**0.35**
S4	InAlGaN	Optimized	’’	302	**0.15**

Figure1: Overview of the four samples showing the phase separation in the metallic area, from the high annular imaging of the scanning TEM, the bright contrast corresponds to large mean Z phases. a)S1: Visible phase separation and Ti rich inclusions (I) inside GaN, b) S2: the Ti rich phases are limited at the interface region, c) S3 Some precipitation along dislocation line (white line), d) S4, clean interface area with small precipitates at the interface.

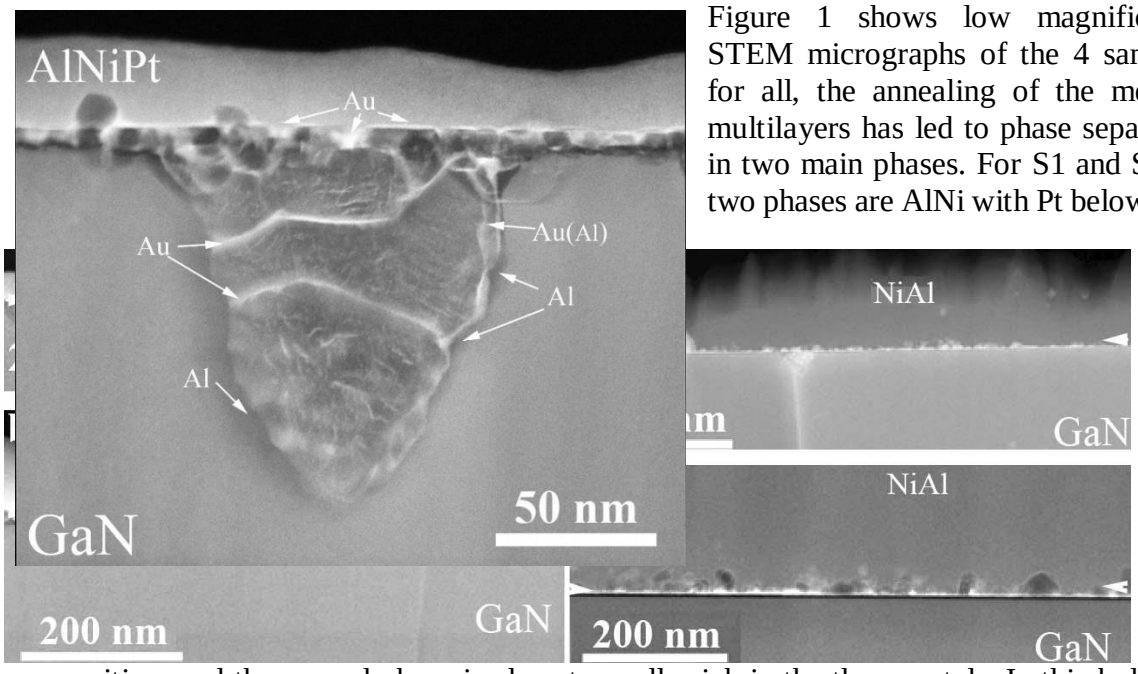

Figure 1 shows low magnification STEM micrographs of the 4 samples, for all, the annealing of the metallic multilayers has led to phase separation in two main phases. For S1 and S2 the two phases are AlNi with Pt below 10% composition, and the second phase is almost equally rich in the three metals. In this bulk part of the metal contact, Au does not contribute, all the EDS analyses show its absence.

Figure 2. S1: Interfacial phases at the nitride metal contact interface, the large Ti rich inclusion is not uniform in image contrast.

The interface area with a large Ti rich inclusion is shown in figure 2. As can be seen, their contrast in not uniform. First, the interfacial area is made of multiple metallic phases, which are topped by a thin Au film just under the AlNiPt phase. The Ti rich inclusion runs then deep inside the GaN template down to around 200 nm. Its contrast is not homogeneous, numerous

bright features cross it in various directions. EDS analysis shows that such areas are rich in Au, and also contain some Al (see arrows which point to the largest ones).

As exhibited in table 1, the measured contact resistance in S2 is below 0.4 Ω.mm and in comparison to S1, the interface morphology and phase distribution has gone important changes. Of course, the phase separation in the bulk is similar to what took place in S1 and this is understood in terms of same annealing conditions and metallic multilayer. Interestingly, in S2, the interface reaction phases extend only to around 70 nm instead of more than 200 nm in the case of S1. Instead of the Ti inclusions that run deep inside the GaN template, three zones can be determined for this interface extension. In zone 1, sporadic crystalline phases protrude inside the top metallic phases of the ohmic contact. Zone II is made of manly Ti rich precipitates that can be identified as TiN; they are imbedded in an Au rich layer on the top and bottom, some of them can slightly protrude inside the GaN template by 10-20 nm (vertical arrow). Underneath this precipitation layer as can be seen in figure 3, thin elongated features can be seen in the basal plane (III), they are just under the bottom Au belt of the Ti rich phases. From the EDS analysis, the not only contain Ti, but also Al and Au.

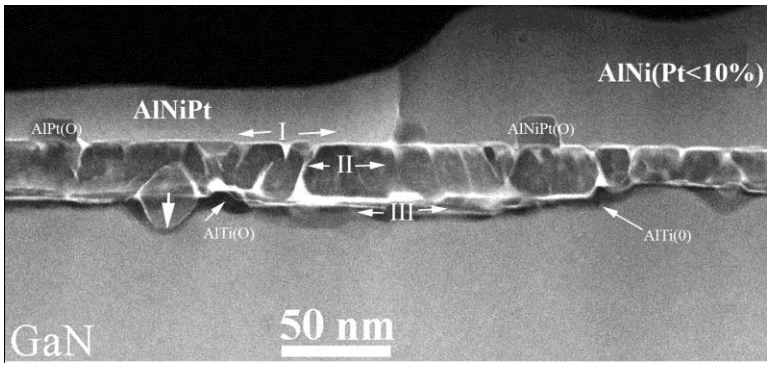

Figure 3: S2, An overview of the phases in sample S2 with their location shown by arrows

Some features need to be pointed out, as illustrated in figure 3, the precipitates that protrude into the metallic phases in zone I are of similar composition but with oxygen. In zone III, the darkest areas are rich in Al and my also contain Ti. The crystallography of area II is interesting, as can be see (fig. 4). As viewed along the [11-20] zone axis of GaN, the TiN crystallites which constitutes the main part of the phases are oriented along the [110] zone axis

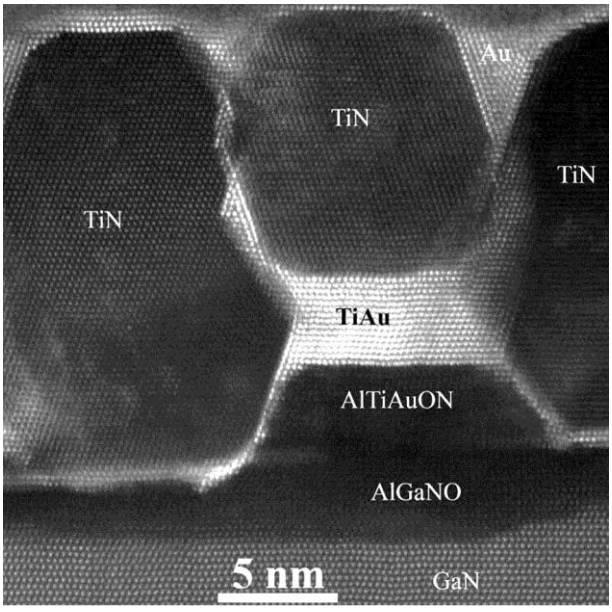

Figure 4: The structure and phases as distributed in the corresponding 50 nm thickness

They all are surrounded by a cubic phase which is rich in Au. Towards the interface with GaN, the phases terminate with some AlGaN which can be oxidized.

The microstructure of S3 and S4 is mainly similar, so they are discussed simultaneously, and of course it rather different from that of samples S1 and S2. In both samples, the phase separation also occurs in the bulk of the metallic part however two distinct phases equally predominate (NiAl and AuAl), not traces of a ternary phase have been detected as in S1 and S2. As can be seen in figure 5, NiAl are NiAu phases are adjacent, although various precipitates can be noticed in S4 inside the two main phases.

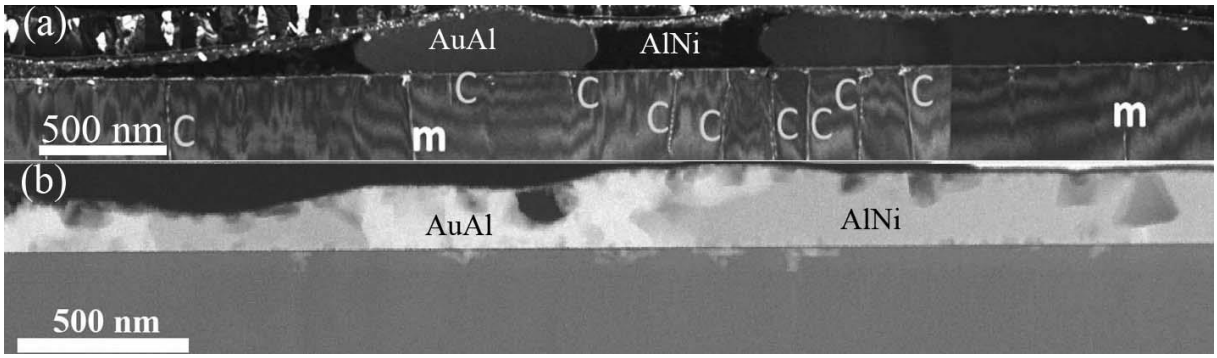

Figure 5: Overviews of samples S3 and S4, a) a weak beam TEM micrograph showing c and mixed type (m) threading dislocations, which are connected to precipitates at the interface with the bulk of the ohmic contact layer. b)The precipitates in S4 are now elongated parallel to the surface of the barrier.

A close examination shows that some difference appears already at this scale between the precipitates at the interface for the two samples. In S3, the precipitates are elongated to follow the threading dislocation line, whereas in S4, they are more extended in the parallel direction of the interface.

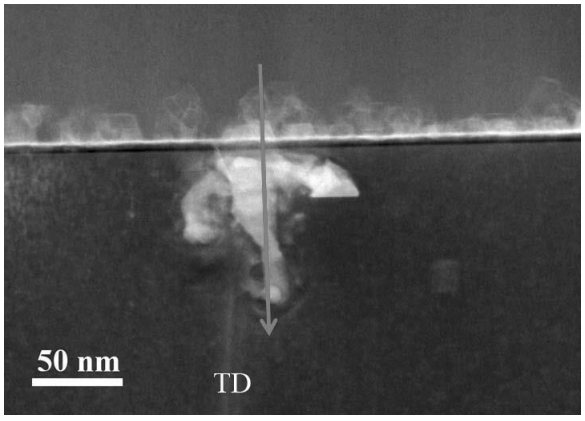

Figure 6: a magnified view of one of the precipitates

The attached dislocation is marked (TD) and other important components of the device are now visible. The dark horizontal narrow band corresponds to the InAlGaN barrier. A bright band is located at its top, just below the numerous small precipitates with have been generated at the bottom of this NiAl phase.

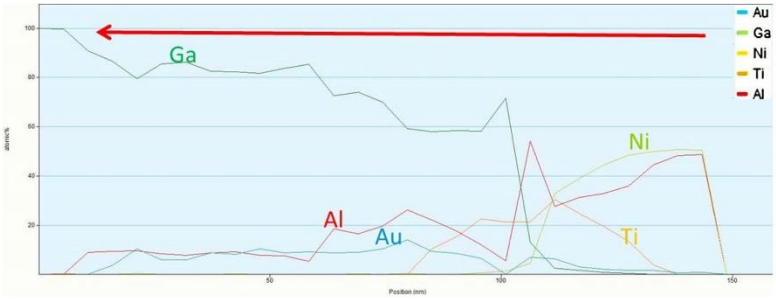

Figure 7, S3: Diffusion profile for the metallic atoms, the arrows indicate the way the data have been recorded

For the above S1 and S2, the interaction with GaN takes place by the formation of Ti rich precipitates, along with the diffusion of Au and Al. In S3, when carrying out EDS analysis, the result is completely different. Going along the line from the NiAl toward the GaN template, it can be seen in figure 7 that first Ni and Al are the only elements of the bulk contact phase. Then the surface precipitates give a mixture of the four elements (Al, Au, Ga, Ni). Ni clearly stops at the interface, and Ti slightly below. Therefore, the observed diffusion connected to dislocation in sample S3 is only due to gold and aluminium atoms. The other feature, which is systematically observed in S3, is the interface structure to the barrier. As can be seen in figure 8, although the bright contrast all along indicates that there is enrichment

in Au, it is very difficult to coincide in lattice fringes between the semiconductor and the metallic part.

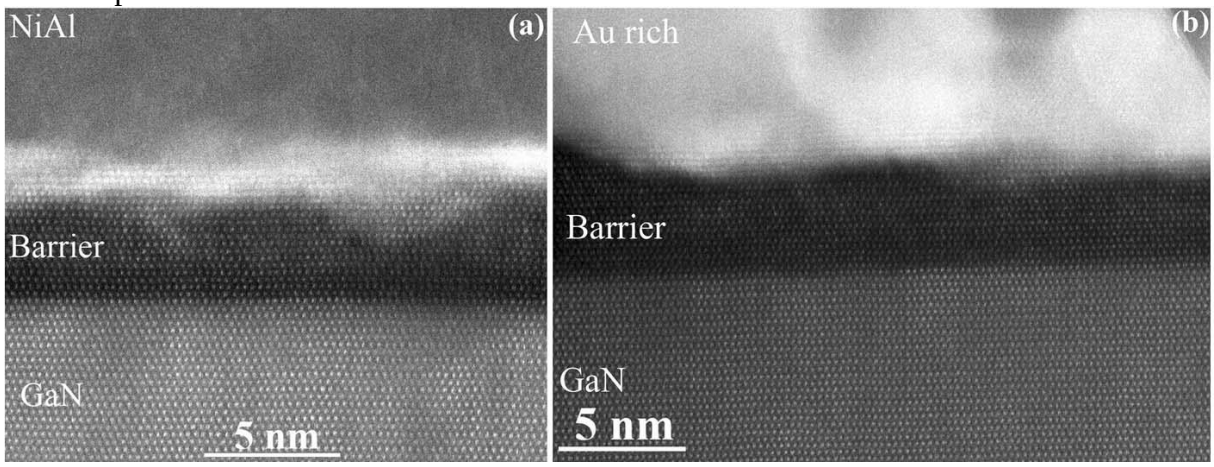

Figure 8, High angle dark field micrograph showing the interface the InAlGaN barrier and the metal contact.

The fact that no lattice fringes are observed inside the metallic part is an indication that no epitaxial relationship exists at this interface, which points out to no coherent crystallographic connection. For S4, the extension of the interfacial reaction of the metal with the semiconductor can be seen in figure 9a which is a magnification of one of the areas of figure 5b. This behaviour is completely different from what has happened in samples S1 and S3 where the inclusions elongate toward the bulk of the GaN template. In this instance, there is no direct formation of individual precipitates that are enriched in one particular metallic element. Instead, the area of diffusion extend parallel to the device surface and except Ni which does not participate in this reaction, the other metals (Au, Al, Ti) are present all over the area (fig. 9b).

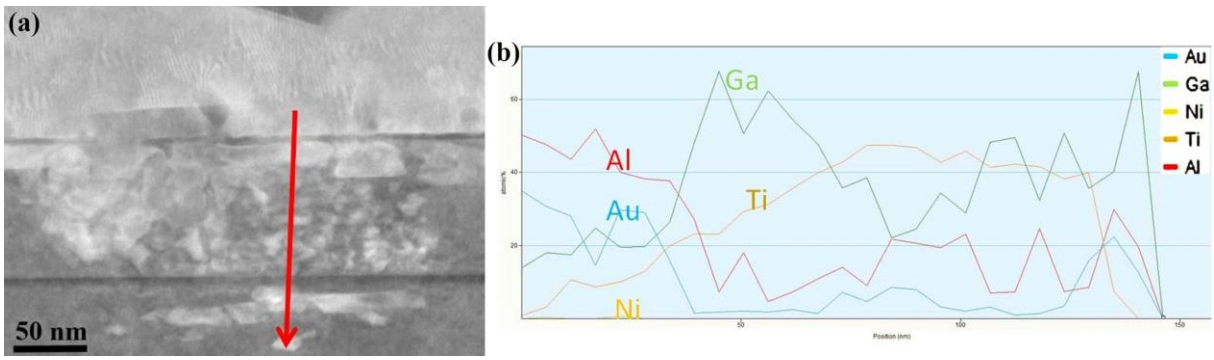

Figure 9. Diffusion reaction at the ohmic contact in sample S4; a) A HAADF micrograph showing the extension of the diffusion of the metals. b) The distribution of the metallic elements as measured by EDS along the red line in figure 9a.

In samples S3 and S4, as can be see in figures 5b and 6a, the interfacial area of the ohmic contact exhibits a large density of small intermetallic precipitates, whereas in S3, no epitaxial relationship can be seen between them and the AlGaInN barrier (fig. 8), the situation is different in S4. As shown in figure 10, the lattice fringes at the top of the barrier are in registry with those of the precipitates. This is valid under the AuAl phase (fig. 10a) as well as in the AlNi rich areas. It is worth to notice that in the AlNi areas the precitates are always imbeded in a gold rich shell (bright contrast in figure 10b)

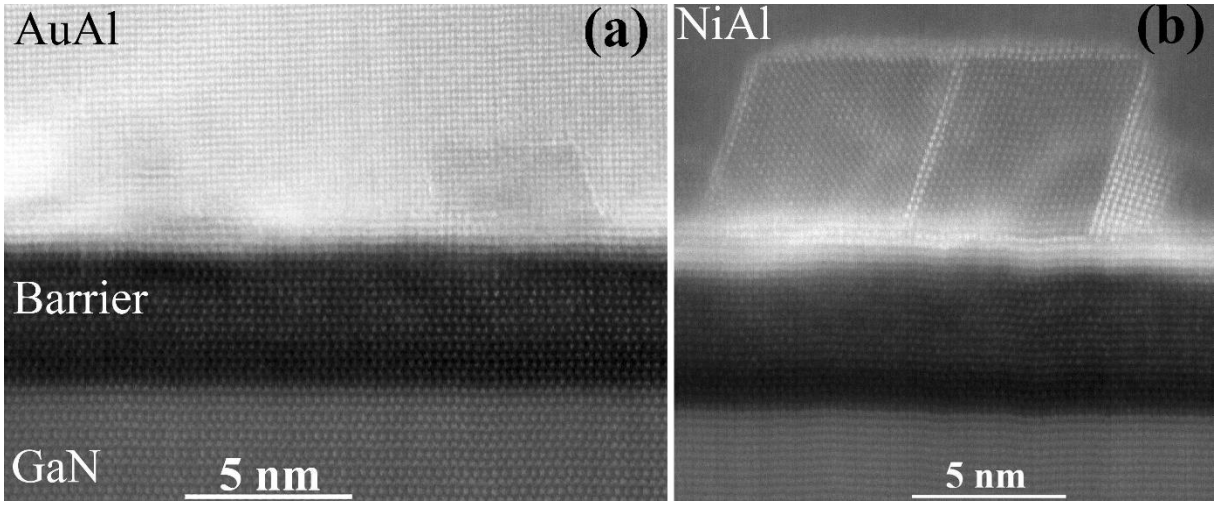

Figure 10. Atomic resolution micrographs of the interface area in Sample S1; a) AuAl area with small precipitates at the interface and a well critalline patch in the intermetallic phase; b) Two well orientated crystallites within a gold rich shell for the NiAl phase.

Summary

In this work, we have investigated the microstructure of ohmic contacts for high electron mobility transistors where the barrier was made of a thin layer of AlGaInN. Samples from two processes for the formation of the ohmic contact have been analysed in a close combination of imaging and chemical analysis down to atomic resolution. Whereas the local microstructure and chemistry alone may not completely explain the electrical behaviour. The above observations show clearly that there may have some relationship. For S1, in which the measured Rc is always above 0.5 Ω.mm, we have large Ti rich inclusions that mostly form along the threading dislocation lines. It should be pointed out that these inclusions are in interaction with Au and Al. In S2 where the ohmic contact is around 0.4 Ω.mm, crystalline Au rich patches surround the 50 nm interfacial zone of nanometric TiN crystallites. The difference between S1 and S2 is then the disappearance of the TiN (Au,Al) inclusions along the dislocation lines. The drop from more than 0.3 to around 1.5 Ω.mm is a large step in the improvement of the ohmic contact and one explanation that taken from the above investigation is also the high crystalline quality of interface with the AlGaN barrier as obtained in S4.

Acknowledgements: This work was partially supported by the Region Normandie under project PLACANANO, convention 18E01651, the EU community under ECSEL JU, project OSIRIS grant agreement N°: 662322. It also benefited from the support of the ANR under project LHOM (ANR-14-CE26-0022) as well as the LABEX GANEX (project QUAHNIMET) and finally the “Investissements d’avenir” ANR-11-EQPX-0020

References

1. J. Kuzmík, Power Electronics on InAlN/(In)GaN: Prospect for a Record Performance, IEEE Electron Device Letters, VOL. 22, 510(2001).
2. F. Medjdoub and J. Carlin, “Status of the emerging InAlN/GaN power HEMT technology, Elec.Elect. Eng. J., 2, 1 (2008).
3. D.S Lee, O. Laboutin, Y. Cao, W. Johnson, E. Bearm, A. Katterson, M. Schuette, P. Saulnier, D. Kopp, P. Fay and T. Palacios, Phys. Stat. Sol. C, 10, 827 (2013).

4. S. Joglekar, M. Azize, M. Beeler, E. Monroy, and T. Palacios, Impact of recess etching and surface treatments on ohmic contacts regrown by molecular-beam epitaxy for AlGaN/GaN high electron mobility transistors, Appl. Phys. Lett. 109, 041602 (2016).
5. Z. Fan, S. N. Mohammad, W. Kim, Ö. Aktas, A. E. Botchkarev, and Hadis Morkoç, Very low resistance multilayer Ohmic contact to n-GaN, Appl. Phys. Lett. 68, 1672 (1996).
6. S. Ruvimov, Z. Liliental-Weber, J. Washburn, K. J. Duxstad and E. E. Haller, Z.-F. Fan, S. N. Mohammad, W. Kim, A. E. Botchkarev, and H. Morkoc, Microstructure of Ti/Al and Ti/Al/Ni/Au Ohmic contacts for n-GaN.
6. The microstructure of Ti/Al and TiN ohmic contacts to gallium nitride. P. Ruterana, G. Nouet, Th. Kehagias, Ph. Komninou, Th. Karakostas, M.A. di Forte Poisson, F. Huet, Phys. Stat. Solidi (a) 176, 767(1999).
7. B. Van Daele, G. Van Tendeloo, W. Ruythooren, J. Derluyn, M. R. Leys, and M. Germain, The role of Al on Ohmic contact formation on-type GaN and AlGaN, Appl. Phys. Lett. 87, 061905 (2005).
8. A. Motayed, R. Bathe, M. C. Wood, O. S. Diouf, R. D. Vispute, and S. N. Mohammad, Electrical, thermal, and microstructural characteristics of Ti/Al/Ti/Au multilayer Ohmic contacts to -type GaN J. Appl. Phys. 93, 1087(2003).
9. B. Jacobs, M. C. J. C. M. Kramer, E. J. Geluk, and F. Karouta, Optimisation of the Ti/Al/Ni/Au ohmic contact on AlGaN/GaN FET structures, J. Cryst. Growth 241, 15 (2002).
10. R. Gong, J. Wang, S. Liu, Z. Dong, M. Yu, C. P. Wen, Y. Cai, and B. Zhang, Analysis of surface roughness in Ti/Al/Ni/Au Ohmic contact to AlGaN/GaN high electron mobility transistors, Appl. Phys. Lett. 97, 062115 (2010).
11. V. Potin, P. Ruterana, G. Nouet, R.C. Pond, and H. Morkoç, Mosaic growth of GaN on (0001) sapphire : a high resolution electron microscopy and crystallographic study of dislocations from low angle to high angle grain boundaries, Phys. Rev. B 61, 5587(2000).
12. P. Vermaut, G. Nouet, P. Ruterana, Observation of two atomic configurations for the {1-210} stacking fault in wurtzite (Ga, Al) nitrides Appl. Phys. Lett. 74, 694(1999).
13. V. Potin, P. Ruterana and G. Nouet, HREM study of stacking faults in GaN layers grown on sapphire substrate, J. Phys. Condensed Matter 12, 10301(2000).
14. P. Ruterana, V. Potin, B. Barbaray, and G. Nouet, Growth defects in GaN layers on top of (0001) sapphire: a geometrical analysis of the misfit effect, Phil. Mag. A 80,937(2000).
15. L. Wang, F. M. Mohammed, and Ilesanmi Adesida, Dislocation-induced non-uniform interfacial reactions of Ti/Al/Mo/Au ohmic contacts on AlGaN/GaN heterostructure, Appl. Phys. Lett. 87, 141915 (2005).
16. J. Guo, Y. Cao1, C. Lian, T. Zimmermann, G. Li, J. Verma, X. Gao, S. Guo, P. Saunier, M. Wistey, D. Jena1, and H. Xing, Metal-face InAlN/AlN/GaN high electron mobility transistors with regrown ohmic contacts by molecular beam epitaxy, Phys. Status Solidi A 208, 1617 (2011).
17. S. Riedmüller, C. Steinmann, J. Grünenpütt, F. Scholz, and H. Blanck, Improvement of Ohmic Contact for InAlGaN/AlN/GaN HEMTs with Recess Etching, Phys. Status Solidi A 2018, 1700456 Phys. Status Solidi A 215, 1700456(2018).
18. S. Arulkumaran, G. I. Ng, K. Ranjan, C. M. M. Kumar, S. C. Foo, K. S. Ang, S. Vicknesh., S. B. Dolmanan, T. Bhat, and S. Tripathy, Record-low contact resistance for InAlN/AlN/GaN high electron mobility transistors on Si with non-gold metal, Japanese Journal of Applied Physics 54, 04DF12 (2015).